Received: 3 November 2022 | Revised: 3 March 2023 | Accepted: 16 March 2023

IET Intelligent Transport Systems

DOI: 10.1049/itr2.12363

The Institution of Engineering and Technology WILEY

ORIGINAL RESEARCH

Cooperative predictive control for arbitrarily mixed vehicle platoons with guaranteed global optimality

Jingyuan Zhan | Zhen Hua | Liguo Zhang

Key Laboratory of Computational Intelligence and Intelligent Systems, Faculty of Information Technology, Beijing University of Technology, Beijing, China

Correspondence
Liguo Zhang, Key Laboratory of Computational Intelligence and Intelligent Systems, Faculty of Information Technology, Beijing University of Technology, Beijing 100124, China.
Email: zhangliguo@bjut.edu.cn

Funding information
National Natural Science Foundation of China, Grant/Award Numbers: U2233211, 62273014, 61873007; Beijing Nova Program, Grant/Award Number: 20220484133; Beijing municipal college faculty construction plan for outstanding young talents, Grant/Award Number: BPHR202203011; Scientific Research Plan of Beijing Municipal Education Commission, Grant/Award Number: KM202310005032

Abstract

This paper studies the cooperative control problem of a mixed vehicle platoon, which is composed of connected autonomous vehicles (CAVs) and human-driven vehicles (HDVs) in an arbitrary order. An alternating direction method of multipliers (ADMM) based distributed model predictive control (DMPC) algorithm is proposed for CAVs to lead the mixed vehicle platoon travelling in a string with anticipated inter-vehicle spacing and a desired velocity. First, the mixed vehicle platoon is divided into multiple interrelated sub-platoons with any two adjacent sub-platoons having a common CAV, and then a generic model is constructed for each sub-platoon based on the intelligent driver model for HDV and the kinematic model for CAV, respectively. Second, a local MPC controller is designed for each sub-platoon to optimize the control inputs of CAVs with the objective of minimizing the position and velocity errors of all vehicles in the sub-platoon, and then the ADMM is utilized to obtain the global optimal solution among local MPC controllers of all sub-platoons. Finally, numerical simulations and experiments are carried out to verify the effectiveness of the proposed DMPC algorithm, the results of which reveal that it can reduce the computation cost significantly and ensure the control performance comparable to the centralized MPC algorithm.

1 | INTRODUCTION

In recent years, the development of vehicle networking technology provides a new way to solve traffic problems. The platooning of vehicles on the highway, known as the control of vehicle platoons, can improve road safety and traffic efficiency, alleviate traffic congestion and reduce energy consumption [1, 2]. The main goal of platooning is to ensure a group of vehicles travel in a string with a desired velocity and maintain an anticipated inter-vehicle spacing [3]. It is noticed that most of the existing platoon control schemes focus on pure connected autonomous vehicles (CAVs) [4, 5]. However, the connected automatic driving technology has not been fully applied, so that CAVs are difficult to completely replace human-driven vehicles (HDVs) in a short time. Therefore, there will be a mixed traffic system in which HDVs and CAVs coexist for a long time to come [6]. The complex traffic environment has brought great challenges to the modeling and control of mixed vehicle platoons, which attract extensive attention of scholars at home and abroad [7–9].

Many scholars have carried out in-depth research on modeling mixed vehicle platoons. Zhu et al. [10] proposed a CAV model based on the optimal velocity model (OVM) with adjustable sensitivity and smooth factor, showing that CAVs were more sensitive and could balance the front and back headway in a mixed vehicle platoon in contrast to HDVs with the OVM. However, this study did not establish an overall model for the mixed vehicle platoon. In [11] and [12], although the mixed vehicle platoon models based on the kinematics of HDVs and CAVs were proposed, there is only one CAV at the tail of the mixed platoon following HDVs. Based on the virtual Mass-Spring-Damper (MSD) theory, Jiang et al. [13] established an MSD model to describe the interaction between vehicles in the mixed vehicle platoon. However, these models are merely suited to specific mixed vehicle platoons rather than arbitrarily mixed vehicle platoons. In [14], Huang et al. proposed a model of the mixed vehicle platoon with arbitrary predefined sequence of HDVs and CAVs, where only one simple case with 6 vehicles was addressed. To the best of our knowledge, the modeling

of mixed vehicle platoons with arbitrary arrangement of HDVs and CAVs is unexplored to a large extent.

Another hot research topic is the control for mixed vehicle platoons. Common methods include PID control [15], sliding mode control [16], neural network control [17], and etc. The main limitation of these control methods is that they are unable to deal with state and control constraints. So some scholars have utilized model predictive control (MPC) to address the vehicle platoon control problem [18, 19]. In [20], Liu et al. proved that if HDVs followed reasonable and simple rules and CAVs moved under the motion plans and coordination protocols based on MPC, the safety of the mixed vehicle platoon can be guaranteed. Feng et al. proposed a tube MPC based robust platoon control algorithm for mixed traffic flow in [21]. However, with the number of vehicles in the platoon increasing, the computational burden of the MPC controller dramatically increases, which may not meet the requirements of real-time control.

In order to reduce the computational burden so as to enhance the real-time control performance, the distributed model predictive control (DMPC) has been attracting more attention. In the DMPC framework for mixed vehicle platoons, a local MPC controller is designed for each CAV, and the multiple local controllers coordinate to find solutions for CAVs in the mixed vehicle platoon. In [22], Luo et al. proposed an unknown input observer based approach for distributed tube-based model predictive control of heterogeneous vehicle platoons. Zhao et al. [23] proposed a distributed and cooperative MPC method to minimize the fuel consumption for mixed vehicle platoons and drive the platoons to pass the intersection on a green phase. In most of the existing DMPC schemes for mixed vehicle platoons, each individual CAV is controlled by a local controller independently with the objective to ensure neighborhood traffic safety and mobility. In [24], a cooperative platoon control strategy based on a modified dual-based distributed MPC algorithm was proposed to ensure the mixed platoon smoothness, efficiency, and stability, which nevertheless relied heavily on the properties of the optimizers. Therefore, it is necessary to develop a novel distributed MPC algorithm which can seek a global optimal control law among local MPC controllers subject to local traffic safety and mobility constraints.

In our study, a DMPC algorithm based on alternating direction method of multipliers (ADMM) is proposed to solve the control problem of a arbitrarily mixed vehicle platoon, where the ADMM has proved to be suitable for large-scale distributed optimization problems with explicit convergence rate in [25, 26]. First, the mixed vehicle platoon is divided into multiple sub-platoons according to the spatial positions of CAVs, and a generic model is proposed for each sub-platoon based on the kinematics of HDVs and CAVs with variable parameters. Second, an MPC based optimization problem for each sub-platoon is established by minimizing inter-vehicle spacing, velocity errors and the acceleration of the CAVs within a finite horizon in the corresponding sub-platoon. Then the global optimization problem of the mixed vehicle platoon is solved by the DMPC controller for each sub-platoon using ADMM from a global perspective. The main contributions of this paper are as follows.

(a) A generic model for the mixed vehicle sub-platoon is constructed based on the linear models of HDVs and CAVs, in which the driving behavior of HDV is described by the intelligent driver model (IDM) [27] and CAV adopts a simplified kinematic model. Distinguished from the existing work [11–13], the mixed vehicle sub-platoon model can be well suited to any mixed vehicle platoon consisting of arbitrary number and sequence of HDVs and CAVs, by dividing the whole platoon into multiple sub-platoons according to the spatial positions of CAVs.
(b) A novel DMPC algorithm based on the ADMM is proposed for the control of an arbitrarily mixed vehicle platoon. Since it has been theoretically proved in [25] that the ADMM can achieve the global optimal solution, the proposed DMPC algorithm ensures the global optimal control of the mixed vehicle platoon in contrast to the DMPC algorithms in [23, 24], which is also verified by numerical simulations and experiments in this paper.

The rest of this paper is organized as follows. In Section 2, we propose a method of decomposing an arbitrarily mixed vehicle platoon into multiple sub-platoons, and then give a generic model for each sub-platoon based on the kinematics of HDVs and CAVs with variable parameters. The ADMM based DMPC algorithm for the mixed vehicle platoon control is presented in Section 3, and the numerical simulation and experimental results are given in Section 4 to verify the effectiveness and superiority of the proposed DMPC algorithm. Finally, conclusions of this paper are made in Section 5.

Notations. The superscript T stands for matrix transposition. I denotes the identity matrix with appropriate dimensions, and $\mathbf{1}_n$ represents an n-dimensional column vector with all entries equal to one. $\otimes$ is the Kronecker product. Given an n-dimensional column vector x, $\|x\|_2 = \sqrt{\sum_{i=1}^{n} x_i^2}$.

2 | MODELING OF A MIXED VEHICLE PLATOON

In this section, we establish a modeling approach for a mixed vehicle platoon, which consists of an arbitrary number of HDVs and CAVs in an arbitrary order. Before modeling the mixed vehicle platoon, the car-following behaviors of both HDVs and CAVs in non-emergency situations are described by the IDM and a simplified kinematic model, respectively.

2.1 | Human-driven vehicle dynamics

The behavior of HDVs in the mixed vehicle platoon is not constrained by the platoon control system designed in this paper. More explicitly, the human driver makes driving decisions according to the velocity of the vehicle itself and its predecessor, as well as the inter-vehicle spacing between the vehicle itself and its predecessor. The popular IDM [27, 28] is adopted to describe

the driving behavior of HDVs, and it can be expressed as:

$$\begin{aligned}\dot{h}_j &= v_{j-1} - v_j,\\ \dot{v}_j &= a\left(1 - \left(\frac{v_j}{v_0}\right)^4 - \left(\frac{s_0 + T_j v_j - \dot{h}_j v_j/\sqrt{4ab}}{h_j}\right)^2\right),\end{aligned} \tag{1}$$

where v_j stands for the velocity of vehicle j in the mixed vehicle platoon, and h_j is the inter-vehicle spacing between vehicle j and its predecessor $j-1$. The parameter a is the maximum acceleration of vehicle j, b is the comfortable deceleration, v_0 is the maximum velocity, s_0 denotes the minimum stopping distance, and T_j is the safe headway time of vehicle j. By adjusting these parameters, different driving behaviors of different human drivers can be expressed.

When the mixed vehicle platoon reaches equilibrium, it is obvious that the velocity of all HDVs in the platoon should be consistent, and each vehicle should keep the desired inter-vehicle spacing from its predecessor. We assume that the constant velocity and the desired inter-vehicle spacing of each vehicle j are v^* and h_j^*, respectively. The relation between h_j^* and v^* is expressed as

$$h_j^* \equiv \frac{s_0 + T_j v^*}{\sqrt{1 - (v^*/v_0)^4}}. \tag{2}$$

Suppose the system is around the equilibrium point (v^*, h_j^*), and define small errors of the velocity and inter-vehicle spacing of any vehicle j as

$$\Delta v_j = v_j - v^*, \Delta h_j = h_j - h_j^*. \tag{3}$$

After performing taylor expansion of (1) around the system equilibrium (v^*, h_j^*) and ignoring the high-order terms, we obtain the following linear differential equation:

$$\begin{bmatrix}\Delta\dot{h}_j\\ \Delta\dot{v}_j\end{bmatrix} = F_j^{\mathrm{HDV}}\begin{bmatrix}\Delta h_j\\ \Delta v_j\end{bmatrix} + G_j^{\mathrm{HDV}}\begin{bmatrix}\Delta h_{j-1}\\ \Delta v_{j-1}\end{bmatrix}, \tag{4}$$

with

$$F_j^{\mathrm{HDV}} = \begin{bmatrix}0 & -1\\ k_{1,j} & k_{3,j}\end{bmatrix}, G_j^{\mathrm{HDV}} = \begin{bmatrix}0 & 1\\ 0 & k_{2,j}\end{bmatrix},$$

where

$$k_{1,j} = \frac{2a\left(s_0 + T_j v^*\right)^2}{\left(h_j^*\right)^3}, k_{2,j} = \frac{\sqrt{a}v^*\left(s_0 + T_j v^*\right)}{\sqrt{b}\left(h_j^*\right)^2},$$

$$k_{3,j} = -\frac{4a(v^*)^3}{(v_0)^4} - \frac{2aT_j\left(s_0 + T_j v^*\right)}{\left(h_j^*\right)^2} - k_{2,j}.$$

2.2 | Connected autonomous vehicle dynamics

As the controllable units in the mixed vehicle platoon, CAVs follow the control law designed in this study. The model of CAVs can be defined as

$$\begin{aligned}\dot{h}_j &= v_{j-1} - v_j,\\ \dot{v}_j &= u_j,\end{aligned} \tag{5}$$

where u_j represents the control input for CAV j, that is, the acceleration of CAV j.

CAVs should achieve the same equilibrium velocity v^* as HDVs in the mixed vehicle platoon, and the constant time-headway policy (CTH) is adopted with the desired inter-vehicle spacing h_j^* for CAV j defined as

$$h_j^* = \tau_j v^* + \bar{h}_j, \tag{6}$$

where τ_j is the constant time-headway for CAV j, and $\bar{h}_j$ is the minimum stopping distance.

Referring to the definitions of the velocity error and inter-vehicle spacing error in (3), the error dynamics for CAVs is formulated as:

$$\begin{bmatrix}\Delta\dot{h}_j\\ \Delta\dot{v}_j\end{bmatrix} = F_j^{\mathrm{CAV}}\begin{bmatrix}\Delta h_j\\ \Delta v_j\end{bmatrix} + G_j^{\mathrm{CAV}}\begin{bmatrix}\Delta h_{j-1}\\ \Delta v_{j-1}\end{bmatrix} + b_j u_j, \tag{7}$$

where

$$F_j^{\mathrm{CAV}} = \begin{bmatrix}0 & -1\\ 0 & 0\end{bmatrix}, G_j^{\mathrm{CAV}} = \begin{bmatrix}0 & 1\\ 0 & 0\end{bmatrix}, b_j = \begin{bmatrix}0\\ 1\end{bmatrix}.$$

$$\dot{X}_i(t) = \underbrace{\begin{bmatrix}F_1^i & & & \\ G_2^i & F_2^i & & \\ & \ddots & \ddots & \\ & & G_{n_i}^i & F_{n_i}^i\end{bmatrix}}_{A_i^t} X_i(t) + \underbrace{\begin{bmatrix}b_1^i & & \\ & \ddots & \\ & & b_{n_i}^i\end{bmatrix}}_{B_{cu}^i}\underbrace{\begin{bmatrix}u_1^i\\ \vdots\\ u_{n_i}^i\end{bmatrix}}_{U_i(t)} + \underbrace{\begin{bmatrix}G_1^i\\ 0\\ \vdots\\ 0\end{bmatrix}}_{B_{cd}^i}\phi_i(t),\ i \in \{1, \ldots, N\} \tag{8}$$

2.3 | Mixed vehicle platoon dynamics

In this paper, we consider an arbitrary mixed vehicle platoon with an HDV as the leading vehicle, which is assumed to track the desired velocity v^*. We assume that overtaking and

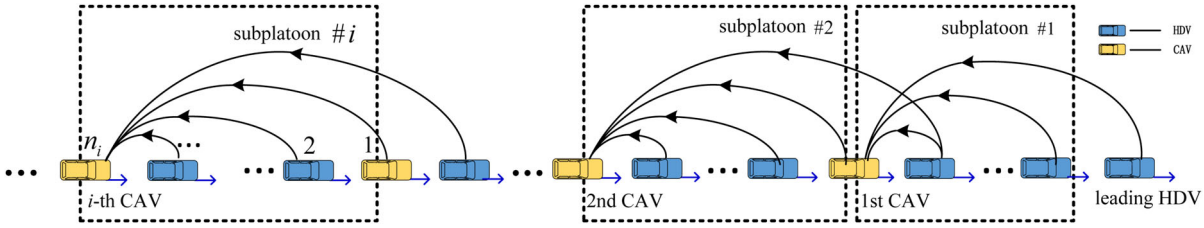

FIGURE 1 The communication topology and the pattern of decomposing the mixed vehicle platoon into multiple sub-platoons, where the blue vehicle represents HDV and the yellow one denotes CAV. Sub-platoon #i corresponds to the i-th CAV. The black arrow represents the wireless communication among the vehicles, and the blue arrow illustrates the vehicle's moving direction.

lane-changing behaviors are prohibited such that the configuration of the mixed vehicle platoon is fixed.

As shown in Figure 1, the mixed platoon is decomposed into multiple interrelated sub-platoons according to the spatial positions of CAVs. Suppose that there are N CAVs in the mixed vehicle platoon, and thus N sub-platoons can be obtained, where sub-platoon #i corresponds to the i-th CAV for any $i = 1, \dots, N$. Sub-platoon #1 covers from the first vehicle behind the leading HDV to the first CAV, and hence we say it is with the HDVs-CAV structure (or it contains only one CAV). For $i = 2, \dots, N-1$, sub-platoon #i covers from the $(i-1)$-th CAV to the i-th CAV, such that it is with the CAV-HDVs-CAV structure or CAV-CAV structure. If the N-th CAV is the tail vehicle of the mixed vehicle platoon, sub-platoon #N is also with the CAV-HDVs-CAV structure or CAV-CAV structure. Otherwise, sub-platoon #N is with the CAV-HDVs-CAV-HDVs structure.

Assume that each CAV receives the information of all vehicles in the corresponding sub-platoon and the preceding vehicle of the sub-platoon via vehicle-to-vehicle (V2V) communication, which is also shown in Figure 1. If the tail vehicle of the mixed vehicle platoon is HDV, the N-th CAV not only receives the information of all vehicles in and the preceding vehicle of sub-platoon #N, but also receives the information of all HDVs behind it.

Remark 1. Suppose that each vehicle is assigned with a sequence number in the platoon and a label to indicate whether it is a CAV or an HDV. At initialization time, each CAV detects the sequence numbers and the label information of its surrounding vehicles, according to which, each CAV i can determine the members of sub-platoon #i so as to settle the communication topology as shown in Figure 1.

Under the communication topology described above, each CAV is capable to establish the model of its corresponding sub-platoon at initialization time. A generic model for all the sub-platoons with different possible structures is constructed with detailed description hereinafter.

Taking sub-platoon #i with n_i vehicles in Figure 1 as an example, the establishment process of the generic model is stated as follows. First, we define

$$x_l^i = \begin{bmatrix} \Delta b_l^i \\ \Delta v_l^i \end{bmatrix}, \tag{9}$$

as the l-th vehicle's state in sub-platoon #i, where $l = 1, 2, \dots n_i$, Δb_l^i and Δv_l^i are the inter-vehicle spacing error and the velocity error of the l-th vehicle in sub-platoon #i, respectively. Then, we define the state vector of sub-platoon #i and the state of the preceding vehicle of sub-platoon #i as

$$X_i = \begin{bmatrix} x_1^i \\ \vdots \\ x_{n_i}^i \end{bmatrix}, \phi_i = \begin{bmatrix} x_{-1}^i \end{bmatrix} = \begin{bmatrix} \Delta b_{-1}^i \\ \Delta v_{-1}^i \end{bmatrix}, \tag{10}$$

respectively.

Next, based on (4) and (7), the generic mixed sub-platoon model is expressed as (10). Matrices $\mathcal{A}_c^i$ and B_{cu}^i are determined by the actual number and sequence of vehicles in the corresponding sub-platoon #i. Specifically, if the l-th vehicle in sub-platoon #i is CAV, F_l^i, G_l^i in $\mathcal{A}_c^i$ and b_l^i in B_{cu}^i are determined by (7). If the l-th vehicle in sub-platoon #i is HDV, F_l^i, G_l^i in $\mathcal{A}_c^i$ are determined by (4), while b_l^i in B_{cu}^i is always zero matrix. Therefore, we have for $l = 1, \dots, n_i$,

$$F_l^i = \begin{cases} F_j^{\text{HDV}}, & \text{if the } l\text{-th vehicle is HDV with index } j \\ F_j^{\text{CAV}}, & \text{if the } l\text{-th vehicle is CAV with index } j \end{cases},$$

$$G_l^i = \begin{cases} G_j^{\text{HDV}}, & \text{if the } l\text{-th vehicle is HDV with index } j \\ G_j^{\text{CAV}}, & \text{if the } l\text{-th vehicle is CAV with index } j \end{cases},$$

$$b_l^i = \begin{cases} \begin{bmatrix} 0 & 0 \end{bmatrix}^T, & \text{if the } l\text{-th vehicle is HDV} \\ \begin{bmatrix} 0 & 1 \end{bmatrix}^T, & \text{if the } l\text{-th vehicle is CAV} \end{cases},$$

$$u_l^i = \begin{cases} 0, & \text{if the } l\text{-th vehicle is HDV} \\ u_j, & \text{if the } l\text{-th vehicle is CAV with index } j \end{cases}.$$

For notational consistence, we define the output and constraint output of sub-platoon #i as

$$Y_{i,c}(t) = X_i(t), \tag{11}$$

and

$$Y_{i,b}(t) = C_b^i X_i(t), \tag{12}$$

respectively. Actually, $Y_{i,c}$ and $Y_{i,b}$ are the state vector of all vehicles in sub-platoon #i and the state vector of all CAVs in

sub-platoon #i, respectively. Obviously, C_b^i in (12) is a $2n_i' \times 2n_i$-dimensional matrix that picks out the components of CAVs, where n_i' denotes the number of CAVs in sub-platoon #i, that is, $n_i' = 1$ or 2. For example, if sub-platoon #i is with the CAV-HDVs-CAV structure, $C_b^i = [1\ 0\ \ldots\ 0\ 1] \otimes I_2$. In addition, the definition of $Y_{i,b}$ is to facilitate the application of safety constraints to CAVs in sub-platoon #i, a detailed description of which can be found in (19).

3 | DMPC FOR MIXED VEHICLE PLATOONS

The objective of mixed vehicle platoon control is to improve traffic efficiency by adjusting the behavior of CAVs, and hence the following performance criteria shall be considered for vehicles in the mixed vehicle platoon.

- Each vehicle needs to reach the desired velocity as soon as possible and keeps a reasonable spacing distance from its predecessor.
- Each CAV needs to minimize fuel consumption during driving.

To achieve the above control objectives, the design and solution of DMPC controllers for the mixed vehicle platoon are presented in this section. DMPC controller $\mathcal{C}_i$ for sub-platoon #i is associated with the i-th CAV, and it can receive the states of all vehicles in sub-platoon #i and the preceding vehicle of sub-platoon #i. Specifically, the DMPC for mixed vehicle platoons mainly includes the following two parts. First, a local optimization problem for each sub-platoon is designed based on DMPC. Second, ADMM is applied to make DMPC controllers solve the control inputs of CAVs in the mixed vehicle platoon from the global perspective.

3.1 | DMPC based optimization problem

Each sub-platoon #i, $i \in \{1, \ldots, N\}$ is assigned with a local controller $\mathcal{C}_i$. We discretize (10) and (11) to obtain the following discrete-time prediction model for the design of controller $\mathcal{C}_i$:

$$\begin{aligned} X_i(k+1) &= \mathcal{A}^i X_i(k) + B_u^i U_i(k) + B_d^i \phi_i(k), \\ Y_{i,c}(k) &= X_i(k), \end{aligned} \tag{13}$$

with

$$\mathcal{A}^i = T\mathcal{A}_c^i + I,\ B_u^i = TB_{cu}^i,\ B_d^i = TB_{cd}^i,$$

where T is the sampling period.

At the current sampling time k, taking the current state of sub-platoon #i as the initial condition, controller $\mathcal{C}_i$ predicts the state of sub-platoon #i on the prediction horizon p and control horizon $m \le p$ based on (13). Then the future output of sub-platoon #i can be expressed as

$$\hat{Y}_{i,c}(k) = \hat{\mathcal{A}}^i X_i(k) + \hat{B}_u^i \hat{U}_i(k) + \hat{B}_d^i \hat{\phi}_i(k) \tag{14}$$

with

$$\hat{Y}_{i,c}(k) = \left[Y_{i,c}^T(k+1|k) \cdots Y_{i,c}^T(k+p|k) \right]^T,$$

$$\hat{U}_i(k) = \left[U_i^T(k|k) \cdots U_i^T(k+m-1|k) \right]^T,$$

$$\hat{\phi}_i(k) = \left[\phi_i^T(k|k) \cdots \phi_i^T(k+p-1|k) \right]^T,$$

$$\hat{\mathcal{A}}^i = \left[(\mathcal{A}^i)^T \cdots ((\mathcal{A}^i)^p)^T \right]^T,$$

$$\hat{B}_u^i = \begin{bmatrix} B_u^i & & \\ \vdots & \ddots & \\ (\mathcal{A}^i)^{m-1} B_u^i & \cdots & B_u^i \\ (\mathcal{A}^i)^m B_u^i & \cdots & \mathcal{A}^i B_u^i + B_u^i \\ \vdots & & \vdots \\ (\mathcal{A}^i)^{p-1} B_u^i & \cdots & (\mathcal{A}^i)^{p-m} B_u^i + \cdots + B_u^i \end{bmatrix},$$

$$\hat{B}_d^i = \begin{bmatrix} B_d^i & & \\ \vdots & \ddots & \\ (\mathcal{A}^i)^{p-1} B_d^i & \cdots & B_d^i \end{bmatrix},$$

where $\hat{Y}_{i,c}(k)$ represents the inter-vehicle spacing and velocity error values of all vehicles in sub-platoon #i on the prediction horizon p, $\hat{U}_i(k)$ is the control inputs of CAVs in sub-platoon #i on the control horizon m, and $\hat{\phi}_i(k)$ is the inter-vehicle spacing and velocity error of the preceding vehicle of sub-platoon #i on the prediction horizon p. Assume that the state of the preceding vehicle of each sub-platoon #i remains unchanged on the prediction horizon, that is, $\phi_i(k|k) = \cdots = \phi_i(k+p-1|k)$.

Based on the mixed vehicle platoon control objectives, we can transform the control problem of CAVs in sub-platoon #i into an optimization problem concerning the inter-vehicle spacing, velocity errors of all vehicles and the acceleration of CAVs in sub-platoon #i on the prediction horizon p. The private cost function for sub-platoon #i is defined as

$$J_i(\hat{U}_i(k)) = \left\| \Gamma_y \hat{Y}_{i,c}(k) \right\|_2^2 + \left\| \Gamma_u \hat{U}_i(k) \right\|_2^2 \tag{15}$$

with

$$\Gamma_y = \mathrm{diag}\{\Gamma_{y,1}, \ldots, \Gamma_{y,p}\},$$
$$\Gamma_u = \mathrm{diag}\{\Gamma_{u,1}, \ldots, \Gamma_{u,m}\},$$

where matrices Γ_y and Γ_u are the weight matrices corresponding to system outputs and control inputs, respectively. Both Γ_y and Γ_u are positive definite symmetric matrices.

It is worth to add a hard constraint that the control input of any CAV in the mixed vehicle platoon at each time step should

be limited to a range $[u_{\min}, u_{\max}]$. Therefore, we obtain the control input range for all CAVs in sub-platoon $\#i$ on the control horizon m, that is

$$u_{\min} \le u_l^i(k+j|k) \le u_{\max}, \tag{16}$$

where $j = 0, \dots, m-1$, and $l = 1, \dots, n_i'$.

Since the control inputs for HDVs are set zero, it is easy to rewrite Ineq. (16) into the following compact form:

$$\hat{U}_{i,\min} \le \hat{U}_i(k) \le \hat{U}_{i,\max}, \tag{17}$$

with

$$\hat{U}_{i,\min} = u_{\min} \cdot \mathbf{1}_{mn_i},$$
$$\hat{U}_{i,\max} = u_{\max} \cdot \mathbf{1}_{mn_i}.$$

Similarly, we also need to consider the safety constraint of CAVs. The IDM itself ensures that there will be no traffic crashes in the driving process of HDVs. To restrict the movements of CAVs in sub-platoon $\#i$, we also apply the model discretization and p step prediction to (10) and (12), obtaining the future constraint output of sub-platoon $\#i$ as

$$\hat{Y}_{i,b}(k) = \bar{A}^i X_i(k) + \bar{B}_u^i \hat{U}_i(k) + \bar{B}_d^i \hat{\boldsymbol{\phi}}_i(k), \tag{18}$$

with

$$\hat{Y}_{i,b}(k) = \left[Y_{i,b}^T(k+1|k) \ \cdots \ Y_{i,b}^T(k+p|k) \right]^T,$$

$$\bar{A}^i = \left[(C_b^i A^i)^T \ \cdots \ (C_b^i (A^i)^p)^T \right]^T,$$

$$\bar{B}_u^i = \begin{bmatrix} C_b^i B_u^i & & \\ \vdots & \ddots & \\ C_b^i (A^i)^{m-1} B_u^i & \cdots & C_b^i B_u^i \\ \vdots & & \vdots \\ C_b^i (A^i)^{p-1} B_u^i & \cdots & C_b^i (A^i)^{p-m} B_u^i + \cdots + C_b^i B_u^i \end{bmatrix},$$

$$\bar{B}_d^i = \begin{bmatrix} C_b^i B_d^i & & \\ \vdots & \ddots & \\ C_b^i (A^i)^{p-1} B_d^i & \cdots & C_b^i B_d^i \end{bmatrix},$$

where $X_i(k)$, $\hat{U}_i(k)$ and $\hat{\boldsymbol{\phi}}_i(k)$ are the same as those in (14).

The constraints for the inter-vehicle spacing and velocity of an arbitrary CAV j are $h_j \ge \tau_{\min} v_j + \bar{h}_j$ and $v_{\min} \le v_j \le v_{\max}$, respectively. $\tau_{\min}$ denotes the minimum safe time-headway for all CAVs. Then the inter-vehicle spacing and velocity error constraints for each CAV can be formulated into the following linear inequality:

$$y_b^{\min} \le D \begin{bmatrix} \Delta h_j \\ \Delta v_j \end{bmatrix} \le y_b^{\max},$$

where D is a 2×2-dimensional constant matrix, $y_b^{\min}$ and $y_b^{\max}$ are 2×1-dimensional constant vectors. Referring to the process of establishing control constraint (17), the state constraint for all CAVs in sub-platoon $\#i$ at each time step, including the inter-vehicle spacing and velocity error constraints on the prediction horizon p, can be defined as

$$\hat{Y}_{i,b}^{\min} \le \hat{D} \hat{Y}_{i,b}(k) \le \hat{Y}_{i,b}^{\max}, \tag{19}$$

where $\hat{D} = I_{n_i' p} \otimes D$ is a $2n_i' p \times 2n_i' p$-dimensional matrix,

$$\hat{Y}_{i,b}^{\min} = \mathbf{1}_{pn_i'} \otimes y_b^{\min},$$
$$\hat{Y}_{i,b}^{\max} = \mathbf{1}_{pn_i'} \otimes y_b^{\max}.$$

Based on further derivations, we obtain the safety constraint related only to independent variables $\hat{U}_i(k)$ according to (18) and (19):

$$\begin{bmatrix} \hat{D}\bar{B}_u^i \\ -\hat{D}\bar{B}_u^i \end{bmatrix} \hat{U}_i \le \begin{bmatrix} \hat{Y}_{i,b}^{\max} - \hat{D}\bar{B}_d^i \hat{\boldsymbol{\phi}}_i - \hat{D}\bar{A}^i X_i \\ \hat{D}\bar{B}_d^i \hat{\boldsymbol{\phi}}_i + \hat{D}\bar{A}^i X_i - \hat{Y}_{i,b}^{\min} \end{bmatrix}. \tag{20}$$

To sum up, we have constructed a local optimization problem for sub-platoon $\#i$ at the current time step k, which is to minimize its private cost function (15) under control constraint (17) and safety constraint (20). Since sub-platoon $\#i$ and its adjacent sub-platoon $\#(i+1)$ cover the same CAV in the mixed vehicle platoon, the corresponding DMPC controllers $\boldsymbol{C}_i$ and $\boldsymbol{C}_{i+1}$ both calculate the control input of that CAV. However, the actual action of that CAV depends on its associated controller $\boldsymbol{C}_i$. At each time step, if $\boldsymbol{C}_i$ solves its private MPC optimization problem independently without coordination with $\boldsymbol{C}_{i+1}$, the control inputs of that CAV given by $\boldsymbol{C}_i$ and $\boldsymbol{C}_{i+1}$ are not necessarily consistent. If this inconsistency is ignored and the control input solved by its on-board controller $\boldsymbol{C}_i$ is directly acted on that CAV, the global optimality can not be guaranteed.

In order to avoid such defect, we further focus on coming up with a distributed optimization algorithm for all DMPC controllers to achieve consistent control inputs for CAVs.

3.2 | ADMM based DMPC algorithm

In this subsection, we propose a DMPC algorithm via ADMM, which provides a distributed solution based on communication among the DMPC controllers for achieving the global optimality.

First, we define a global variable

$$\hat{Z}(k) = [Z^T(k|k) \ \dots \ Z^T(k+m-1|k)]^T$$

as the control inputs of all CAVs in the mixed vehicle platoon on the control horizon m at each time step k, where $Z = [Z_1 \ \dots \ Z_N]^T$ with $Z_i, i = 1, \dots, N$ denoting the control input for the i-th CAV. We also introduce an auxiliary variable $\tilde{Z}_i$ to be the global variable's idea of what the local variable $\hat{U}_i$ should be. Obviously, $\tilde{Z}_i$ consists of the components of $\hat{Z}$ corresponding to the CAVs in sub-platoon $\#i$ and all zero entries for HDVs, such that it can be written as a linear function of Z, that

is, $\tilde{Z}_i = \hat{P}_i\hat{Z}$ with $\hat{P}_i = I_m \otimes P_i$. For example, if sub-platoon $\#i$ is with the CAV-HDVs-CAV structure, P_i is a $n_i \times N$-dimensional matrix with $P_i(1, i-1) = P_i(n_i, i) = 1$ and all the other entries equal to 0.

Then we define a global cost function for the mixed vehicle platoon at time step k as

$$J\big(\hat{Z}(k)\big) = \sum_{i=1}^{N} J_i\big(\hat{P}_i\hat{Z}(k)\big),\ \hat{P}_i\hat{Z}(k) \in \Omega_i, \tag{21}$$

where $J_i(\hat{P}_i\hat{Z}(k))$ is the private cost function induced by $\tilde{Z}_i$ for sub-platoon $\#i$ as defined in (15), and Ω_i is the feasible set for control inputs of sub-platoon $\#i$ satisfying constraints (17) and (20). Combining (14), the global cost function (21) of the mixed vehicle platoon can be written into the following standard form:

$$J\big(\hat{Z}(k)\big) = \sum_{i=1}^{N}\left(\frac{1}{2}(\hat{P}_i\hat{Z}(k))^T H_i\hat{P}_i\hat{Z}(k) + f_i^T\hat{P}_i\hat{Z}(k)\right),\quad \hat{P}_i\hat{Z}(k) \in \Omega_i, \tag{22}$$

where

$$H_i = 2((\hat{B}_u^i)^T\Gamma_y\hat{B}_u^i + \Gamma_u),$$

$$f_i = (2E_i^T\Gamma_y\hat{B}_u^i)^T,$$

with

$$E_i = \hat{A}^i X_i + \hat{B}_d^i\hat{\phi}_i.$$

To realize the global optimality in terms of (22), DMPC controllers need to coordinate to find $\hat{U}_i$ satisfying

$$\hat{U}_i - \tilde{Z}_i = 0, i = 1, \dots, N. \tag{23}$$

Hence, we construct an augmented Lagrange function as

$$\begin{aligned} &L_\rho\big(\{\hat{U}_i\}_{i=1}^N, \{\tilde{Z}_i\}_{i=1}^N, \{\lambda_i\}_{i=1}^N\big) \\ =\ &\sum_{i=1}^{N}\left(J_i(\hat{U}_i) + \lambda_i^T\big(\hat{U}_i - \tilde{Z}_i\big) + \frac{\rho_i}{2}\big\|\hat{U}_i - \tilde{Z}_i\big\|_2^2\right). \end{aligned} \tag{24}$$

For finding the minimum value of function (24), it is necessary to determine $\hat{U}_i, \lambda_i$ and $\tilde{Z}_i$. ADMM allows computing $\hat{U}_i, \lambda_i$ and $\tilde{Z}_i$ in parallel. On each DMPC controller, the minimum value of (24) is obtained by the alternating optimization of these variables. When updating one of the variables, other variables are regarded as constant values. The iterative calculation process on $\mathcal{C}_i$ under the ADMM framework is described as follows.

3.2.1 | Update of $\hat{U}_i$

According to the values of λ_i^γ and $\tilde{z}_i^\gamma$ obtained by $\mathcal{C}_i$ in the $(\gamma-1)$-th iteration, the updating of $\hat{U}_i$ can be performed on

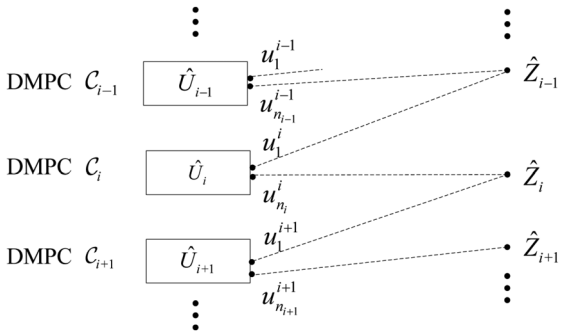

FIGURE 2 The corresponding relationship between the components of local variables $\{\hat{U}_i\}_{i=1}^N$ and global variable $\hat{Z}$ when control horizon $m = 1$.

$\mathcal{C}_i$ by solving the private constrained optimization problem of sub-platoon $\#i$, which is described as

$$\hat{U}_i^{\gamma+1} = \arg\min_{\hat{U}_i}\left(J_i(\hat{U}_i) + \lambda_i^{\gamma T}\hat{U}_i + \frac{\rho_i}{2}\left\|\hat{U}_i - \tilde{Z}_i^\gamma\right\|_2^2\right)\quad \hat{U}_i \in \Omega_i, i = 1, \dots N. \tag{25}$$

3.2.2 | Update of $\tilde{Z}_i$

Due to $\tilde{Z}_i = \hat{P}_i\hat{Z}$, the update of $\tilde{Z}_i$ can be transformed into the update of the global variable $\hat{Z}$. Considering $\hat{Z}(k) = [Z^T(k|k) \quad \dots \quad Z^T(k+m-1|k)]^T$ and $\hat{U}_i(k) = [U_i^T(k|k) \ \dots \ U_i^T(k+m-1|k)]^T$, we focus on the update rule of $Z(k+j|k)$ from $\{U_i(k+j|k)\}_{i=1}^N$ for any $j = 0, \dots, m-1$. We will leave out $(k+j|k)$ for notational simplicity hereinafter. Since L_ρ is fully separable in its components, the Z-update step decouples across the components of it according to Boyd's derivation in [25]:

$$\begin{aligned} Z_i^{\gamma+1} &= \left(U_i^{\gamma+1}(n_i) + U_{i+1}^{\gamma+1}(1)\right)/2,\ i = 1, \dots, N-1, \\ Z_N^{\gamma+1} &= U_N^{\gamma+1}(r), \end{aligned} \tag{26}$$

where r denotes the index of the second CAV in sub-platoon $\#N$.

Taking the case with control horizon $m = 1$ as an example shown in Figure 2, $\tilde{Z}_i$ is the average of the last component of $\hat{U}_i$ and the first component of $\hat{U}_{i+1}$ for all $i = 1, \dots, N-1$, and $\tilde{Z}_N$ is equal to the component of $\hat{U}_N$ corresponding to the second CAV in sub-platoon $\#N$. In other words, the update of $\tilde{Z}_i$ requires DMPC controllers $\mathcal{C}_i$ and $\mathcal{C}_{i+1}$ to exchange their solutions for all $i = 1, \dots, N-1$.

3.2.3 | Update of λ_i

Dual variables are updated based on the dual ascending method, and the updating rule of λ_i is given by

$$\lambda_i^{\gamma+1} = \lambda_i^\gamma + \rho_i\left(\hat{U}_i^{\gamma+1} - \tilde{Z}_i^{\gamma+1}\right). \tag{27}$$

ALGORITHM 1 DMPC algorithm for mixed vehicle platoon control

% $\gamma_{\max}$: Maximum iterations of ADMM.

for $k = 1, \dots, k_{\max}$ **do**

Combining the current state value $X_i(k)$ and the prediction model (13) of each sub-platoon to predict the future output $\hat{Y}_{i,r}(k)$ of each sub-platoon system, respectively;

According to (15), (17) and (20), establishing the private constrained cost function of each sub-platoon system;

According to (21), establishing the global cost function J of the mixed vehicle platoon system;

Randomly initialize $\hat{U}_i^0(k)$, $\bar{Z}_i^0(k)$, $\lambda_i^0(k)$ on each DMPC controller;

for $\gamma = 0, \dots, \gamma_{\max} - 1$ **do**

Update $\hat{U}_i^{\gamma+1}(k)$ according to (25) on each DMPC controller parallelly;

DMPC controller $\mathcal{C}_i$ transmits $\hat{U}_i^{\gamma+1}(k)$ to controller $\mathcal{C}_{i-1}$ for all $i = 2, \dots, N$;

Update $\bar{Z}_i^{\gamma+1}(k)$ according to (26) and $\bar{Z}_i = \hat{P}_i \hat{Z}$ with the updated $\hat{U}_i^{\gamma+1}(k)$ and $\hat{U}_{i-1}^{\gamma+1}(k)$ on each DMPC controller parallelly;

Update $\lambda_i^{\gamma+1}(k)$ according to (27) with the updated $\hat{U}_i^{\gamma+1}(k)$ and $\bar{Z}_i^{\gamma+1}(k)$ on each DMPC controller parallelly;

end for

end for

TABLE 1 Parameters of CAVs in the mixed vehicle platoon.

Vehicle type	Vehicle index	Vehicle parameters
CAV	5	$\tau_5 = 1$ s, $\bar{b}_5 = 2$ m
CAV	7	$\tau_7 = 1.2$ s, $\bar{b}_8 = 2$ m
CAV	11	$\tau_{11} = 1.5$ s, $\bar{b}_{11} = 2$ m
CAV	14	$\tau_{14} = 1.8$ s, $\bar{b}_{14} = 2$ m
CAV	15	$\tau_{15} = 1.2$ s, $\bar{b}_{17} = 2$ m
CAV	20	$\tau_{20} = 2.0$ s, $\bar{b}_{20} = 2$ m

The same as the update of $\hat{U}_i$, the update of λ_i is carried out independently on DMPC controller $\mathcal{C}_i$.

3.2.4 | Stopping criteria

After updating the related variables, the next iteration can be carried out. The above iterative calculation process is repeated on each DMPC controller until the maximum number of iterations preset by the algorithm is reached, and all the on-board DMPC controllers output the control inputs to act on the corresponding CAVs in the mixed vehicle platoon.

In summary, the ADMM based DMPC algorithm for mixed vehicle platoon control is given explicitly in Algorithm 1. Under the framework of ADMM, the DMPC controllers find the optimal solution of (22) through parallel computing and coordination, such that the global optimality of the mixed vehicle platoon control system is ensured.

TABLE 2 Parameters of reference IDM.

Parameters	Value	Parameters	Value
a	1 m/s^2	v_0	33.3 m/s
s_0	2 m	b	2.8 m/s^2

TABLE 3 T_j of different HDVs in the mixed vehicle platoon.

Vehicle index	T_j	Vehicle index	T_j
1, 2, 3, 4	1.5 s	6	1.6 s
8, 9, 10	1.7 s	12, 13	1.8 s
16, 17	1.9 s	18, 19	2.0 s

4 | SIMULATIONS AND EXPERIMENTS

In this section, MATLAB and robot operating system (ROS) are used to verify the effectiveness and superiority of the proposed DMPC algorithm in both the control performance and computational cost for controlling mixed vehicle platoons.

4.1 | Numerical simulation results based on MATLAB

4.1.1 | Numerical simulation design and parameter selection

In this section, a mixed platoon with 20 vehicles in a single lane is selected as the testbed, which runs in a virtual environment established by using the System Build software package in MATLAB. The movement of the leading vehicle follows the preset velocity curve, which is the reference velocity of the whole mixed vehicle platoon. We let the leading vehicle run at a constant velocity of 30 m/s and begin to slow down at 500 s until reaching a new constant velocity of 25 m/s. Without loss of generality, vehicles 5, 7, 11, 14, 15 and 20 are selected as CAVs, the parameters of which are given in Table 1. The remaining vehicles in the mixed vehicle platoon are HDVs modelled by IDM with different human driver parameters. The related parameters of the reference IDM are shown in Table 2 [28], and the safe time-headways of all HDVs are shown in Table 3. From Tables 1 and 3, we note that the time-headways for both CAVs and HDVs are different. Therefore, the desired inter-vehicle spacings are non-uniform, which is indeed different from the usual case of a uniform desired inter-vehicle spacing. Basically, achieving such non-uniform desired inter-vehicle spacings is more general, and it can also reflect the heterogeneity of vehicles in reality.

Referring to the vehicles' parameters in Tables 1–3, we give the relevant control and safety constraints. The maximum velocity for all CAVs is set as 120 km/h, and the minimum inter-vehicle spacing for any CAV j is set as $\tau_{\min} v_j + \bar{b}_j$ with $\tau_{\min} = 0.5$ s. The upper and lower bounds of the acceleration are $a_{\max} = 1$ m/s^2 and $a_{\min} = -2.8$ m/s^2, respectively.

As previously mentioned, the mixed vehicle platoon system with 20 vehicles is divided into 6 interrelated sub-platoon systems according to the spatial positions of the CAVs. Obviously, these sub-platoon systems are different in the vehicle number and configuration, such that the mixed vehicle platoon could be regarded as a typical example with arbitrary number and sequence of HDVs and CAVs in a certain sense. For each DMPC controller, the sampling period, prediction horizon and control horizon are set as $T = 0.1$ s, $p = 30$ and $m = 20$, respectively. Due to the magnitude difference between the state quantity and the control quantity, the weight ratio of the two in cost function (15) is set to be 1:28, so as to achieve a better control performance on both velocity and inter-vehicle spacing responses.

In order to verify the effectiveness and superiority of the proposed DMPC algorithm for mixed vehicle platoons, we establish three numerical examples for comparison. Examples I and II are carried out for the mixed vehicle platoon with 20 vehicles described above. In example I, the proposed DMPC algorithm is used to control the mixed platoon. In example II, the Centralized MPC (CMPC) algorithm (i.e. minimizing the global cost function (22)) with the same relevant parameters as those of the DMPC algorithm is applied. In example III, the 6 CAVs in the mixed vehicle platoon are replaced by 6 HDVs, whose constant time-headways and minimum stopping distances are with the same values as those of the corresponding CAVs. A detailed analysis of the simulation results among the three numerical examples is given as follows.

4.1.2 | Comparison results in control performance

In order to compare the control performance of the three algorithms more intuitively, we plot the velocity, inter-vehicle spacing and acceleration responses of some vehicles in the three examples in Figure 3. Vehicles 13, 14, 19, and 20 are selected as samples, where CAV 14 and HDV 13 have the same constant time-headway and minimum stopping distance, and so are CAV 20 and HDV 19. The trajectories of different vehicles are distinguished by the color, and the profile of the leading vehicle's velocity is shown in the velocity response with black solid line.

As shown in Figure 3, the safety and control constraints that vehicles in the mixed platoon should satisfy are plot with dotted lines. Since the behaviors of HDVs in the mixed vehicle platoon follow the IDM, the control and safety constraints for HDVs are satisfied naturally. The inter-vehicle spacing, velocity and acceleration responses of CAVs under DMPC and CMPC algorithms show that the constraints for CAVs are also satisfied.

Furthermore, we find that when the velocity of the leading vehicle reaches the equilibrium, CAVs 14 and 20 under CMPC and DMPC algorithms can also achieve the same velocity and maintain the desired inter-vehicle spacing, which indicates that the control goal is achieved. In more detail, it can be observed that CAV 14 achieves a smaller inter-vehicle spacing than HDV 13 with the same constant time-headway and minimum stopping distance, and the same conclusion apply for CAV 20 and HDV 19, which indicates CAVs can improve the road traffic capacity to a certain extent. On the other hand, CAVs can achieve higher acceleration than HDVs, which means that CAVs are more sensitive to the velocity change of the leading vehicle so as to drive the mixed vehicle platoon to be stable as soon as possible.

To quantitatively compare the platoon control performance under different control algorithms, we define a performance index $\bar{J} = X'QX + U'RU$. In examples I and II, X represents the actual states of all vehicles except the leading vehicle in the mixed vehicle platoon at each time step, including velocity and inter-vehicle spacing errors, and U denotes the actual control inputs of 6 CAVs in the mixed platoon at each time step. Similarly, in example III, X represents the velocity and inter-vehicle spacing errors of 19 HDVs under IDM strategy at each time step, and U is the control inputs actually adopted by the corresponding 6 HDVs at each time step. Figure 4 shows that the values of $\bar{J}$ are all equal to 0 when the system reaches the equilibrium, which means that the DMPC, CMPC and IDM strategies can achieve the platoon control goal. When the system does not reach the equilibrium, the values of $\bar{J}$ under CMPC and DMPC are always much smaller than that under IDM strategy, which indicates that the introduction of CAVs improves the car following performance of traffic flow. More importantly, in the same scenario setting, $\bar{J}$ under DMPC is approximately equal to that under CMPC all the time. In other words, the DMPC algorithm is comparable to CMPC in the platoon control performance, which means that the ADMM has excellent convergence rate, and the control input given by the DMPC algorithm approaches the global optimal solution even under finite iterations in practice.

To quantitatively analyze the car following performance under DMPC, we calculate the average value of velocity variance of 20 vehicles during the whole simulation period in the three examples. This average value can reflect the velocity fluctuation of all vehicles in the mixed platoon during the process of car following. The smaller the average value is, the more stable the overall car following performance is. As shown in Figure 5, $\overline{Var(v)}$ under CMPC and DMPC algorithms are 15.15% and 12.75% smaller than that under IDM strategy, respectively, indicating that the car following performance of mixed vehicle platoon under CMPC and DMPC algorithms is more stable than that of pure HDVs under IDM strategy. Moreover, the car following performance under DMPC is very close to that under CMPC.

4.1.3 | Comparison results in computation cost[1]

To verify the superiority of the DMPC algorithm in reducing computation cost, we calculate the total time cost of CMPC

[1] The DMPC algorithm can be realized by the edge computing unit involving the centralized data storage and distributed computing, such that the information transmission between local controllers is achieved by direct data reading in the unit rather than the wireless communication technology. In this case, we can calculate the computation cost of the proposed DMPC algorithm by ignoring the time spent on the communication among local controllers during the iterative computation process.

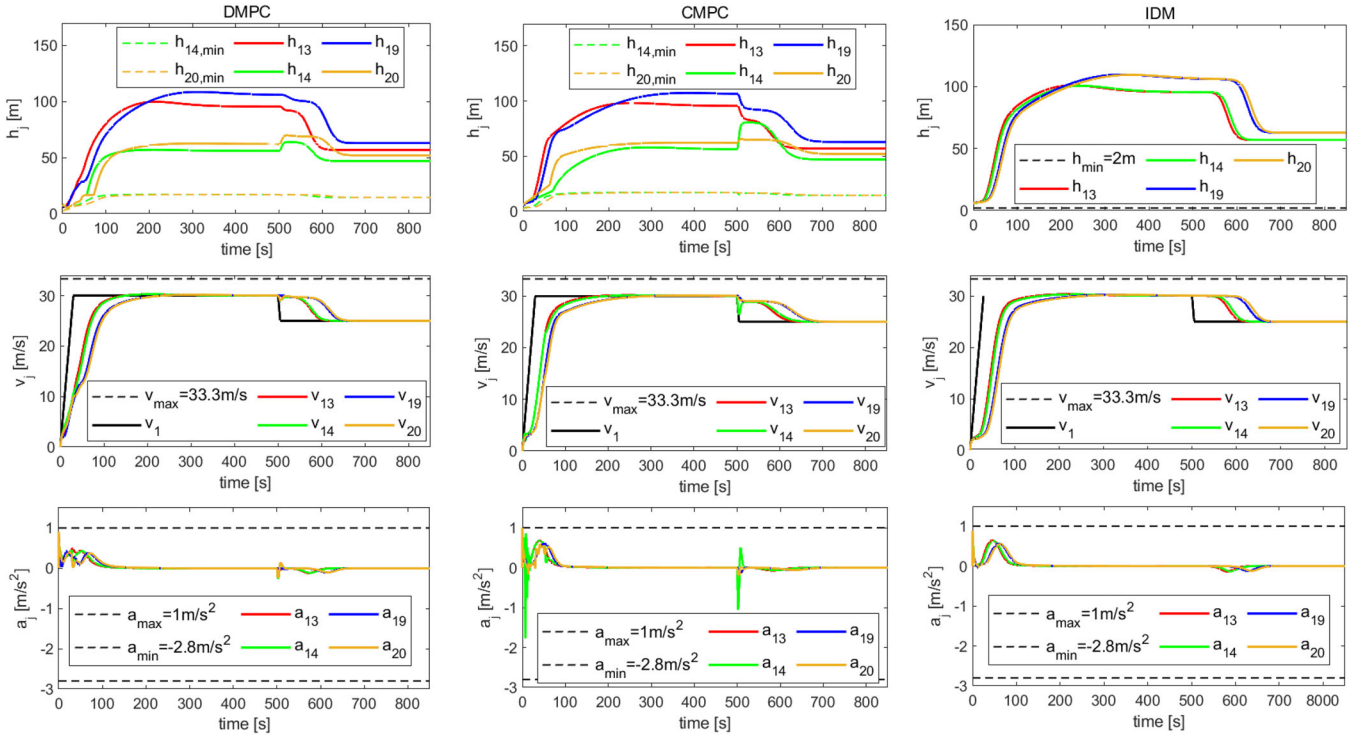

FIGURE 3 Inter-vehicle spacing (the 1st row), velocity (the 2nd row) and acceleration (the 3rd row) responses of some vehicles in the mixed vehicle platoon under three different control strategies. The LHS column corresponds to the DMPC algorithm, the middle column corresponds to the CMPC algorithm, and the RHS column corresponds to the IDM strategy.

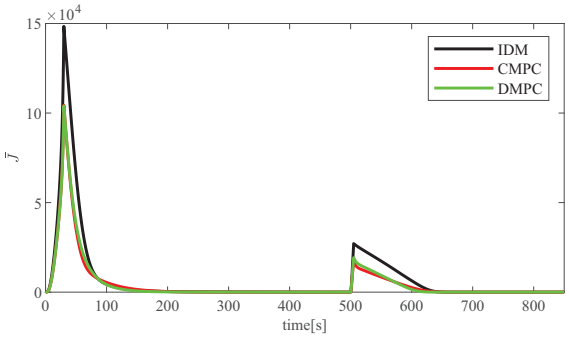

FIGURE 4 The value of control performance index $\bar{J}$ under three control strategies at each time step.

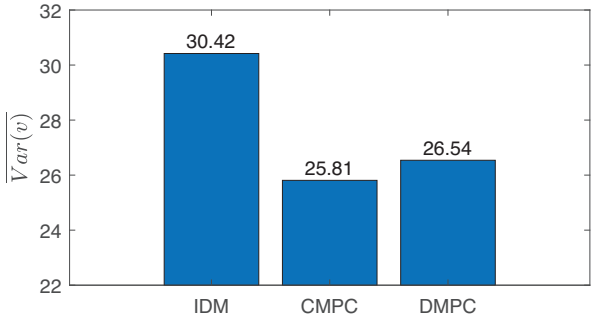

FIGURE 5 The average value of the velocity variance of 20 vehicles in the three examples during the simulation period.

TABLE 4 Calculation time cost ($p = 30$, $m = 20$).

	Total time cost (s)	Average time cost (s)
CMPC	327.46	0.039
DMPC	109.72	0.013

and DMPC algorithms, respectively, in the simulation period, the statistical results of which are shown in Table 4.

Recall that prediction horizon $p = 30$ and control horizon $m = 20$, and the sampling period is 0.1 s. In addition, we set the simulation running time as 850 s, which means there are 8500 times of optimization calculation in both CMPC and DMPC algorithms. As shown in table 4, the total calculation time and the average calculation time at one time step of the CMPC algorithm are about 327.46 s and 0.039 s, respectively. The calculation time of DMPC controllers may be different from each other because sub-platoons are different, and hence we define the time cost of the DMPC algorithm as the maximum calculation time of all DMPC controllers. As shown in table 4, the total calculation time of the DMPC algorithm is 109.72 s, and the average calculation time of the DMPC algorithm is about 0.013 s, which is 66.67% lower than that of the CMPC algorithm.

Furthermore, we compare the computation cost of CMPC and DMPC algorithms when prediction horizon $p = 40$ and control horizon $m = 30$. According to the results shown in

TABLE 5 Calculation time cost ($p = 40$, $m = 30$).

	Total time cost (s)	Average time cost (s)
CMPC	615.23	0.072
DMPC	126.37	0.015

Table 5, the average calculation time of the DMPC algorithm is 79.17% lower than that of the CMPC algorithm, which reveals that the calculation time reduction is more remarkable than the previous case with $p = 30$ and $m = 20$. This is because the computational burden of the CMPC algorithm increases with the prediction horizon of the controller or the number of vehicles in the mixed vehicle platoon, while the computational burden of the DMPC algorithm would not increase with the complexity of optimization problems and the platoon scale that much. In other words, when the computational burden is higher, the advantage of the DMPC algorithm in reducing the computation cost is more obvious.

Particularly, the sampling period is set as 0.1 s, which requires that the controllers solve the optimization problem within 0.1 s. The numerical simulation results show that the CMPC algorithm may not be able to meet the real-time control requirement if the mixed vehicle platoon is with a larger size. In contrast, the DMPC algorithm proposed in this paper is more feasible in actual traffic scenes.

4.2 | Experimental verification with turtlebot3

In order to test the applicability of the proposed DMPC algorithm in the real mixed vehicle platoon, the platoon control experiment is conducted with the wheeled mobile robot turnlebot3 and the 3D motion capture system based on infrared camera. In the experiment, the camera can recognize different robot vehicles through the marked reflective points, and the velocity and position information captured is broadcasted by the server after data processing. At the same time, CAVs and HDVs can receive and transmit motion data through WIFI. Figure 6 is a schematic diagram of the experimental field, which consists of two crooked roads with the radius of 0.65 m and two straight roads with the total length of 1 m. Eight infrared cameras are evenly installed on the surrounding walls. As shown in Figure 6, 11 Turnlebot3 robots are used in the experiment. Turnlebot3 is equipped with Raspberry Pi 3, which can carry out data operation and vehicle control independently. Vehicles 3, 5, 7, and 10 represent CAVs controlled by the DMPC algorithm, and others are HDVs, which are modeled by IDM with consistent parameters. Due to the limitations of the experimental field and the hardware conditions of Turtlebot3, we adjust the vehicle parameters of HDVs as shown in Table 6 except the leading vehicle. The constant headway time and minimum stopping distance of four CAVs are set as 3 s and 0.05 m, respectively.

Let the leading vehicle increase its velocity from 0 m/s to 0.08 m/s at acceleration of 0.01 m/s, according to the

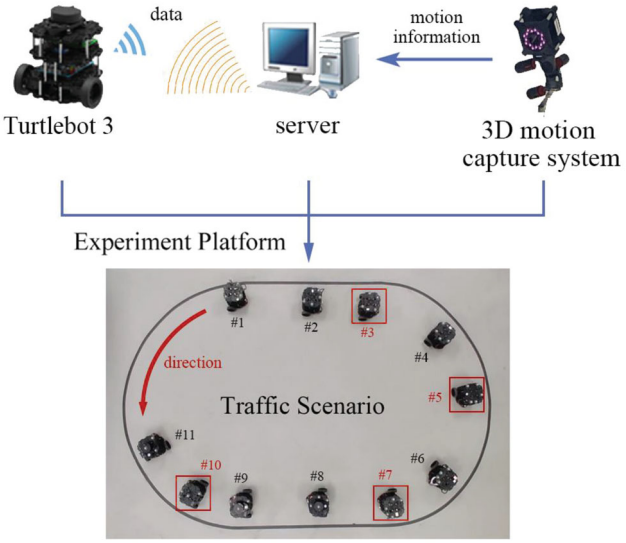

FIGURE 6 Diagram of the experiment platform. In the traffic scenario, vehicles 3, 5, 7, and 10 represent CAVs controlled by DMPC and others are HDVs. The red arrow indicates the movement direction of the 11 robot vehicles.

TABLE 6 Parameters of HDVs in the experiment.

Parameters	Value	Parameters	Value
a	0.01 m/s^2	v_0	0.15 m/s
s_0	0.08 m	T_j	4 s
b	0.05 m/s^2	L	0.14 m

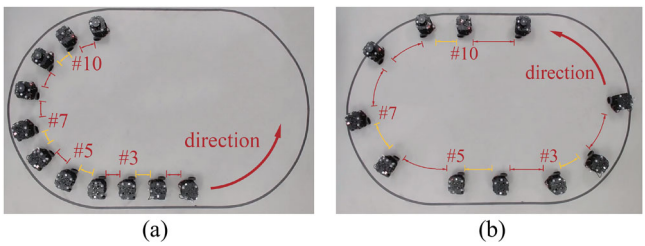

FIGURE 7 The movement process and trajectories of the mixed vehicle platoon with 11 robot vehicles.

parameters of vehicles selected in the experiment. The desired inter-vehicle spacing of HDVs and CAVs are $h_2^* = h_4^* = h_6^* = h_8^* = h_9^* = h_{11}^* = 0.4172$ m and $h_3^* = h_5^* = h_7^* = h_{10}^* = 0.29$ m. Figures 7–9 show the experimental results[2] under the DMPC algorithm from different aspects. Figure 7a shows the initial positions of these vehicles in the traffic scene, and Figure 7b indicates that the mixed vehicle platoon reaches the equilibrium state. Figures 8 and 9 are the velocity and inter-vehicle spacing responses of the 11 vehicles from the initial states to the equilibrium state, where the solid lines represent HDVs and the dotted lines correspond to CAVs.

[2] The complete experimental video can be found at the website https://github.com/Sandyvicmark/DMPC.

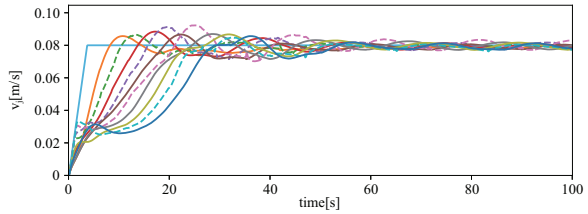

FIGURE 8 Velocity responses of 11 robot vehicles in the real experiment environment.

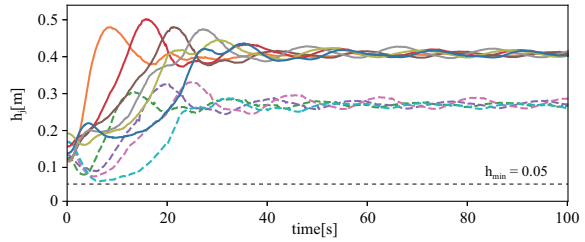

FIGURE 9 Inter-vehicle spacing responses of 11 robot vehicles in the real experiment environment.

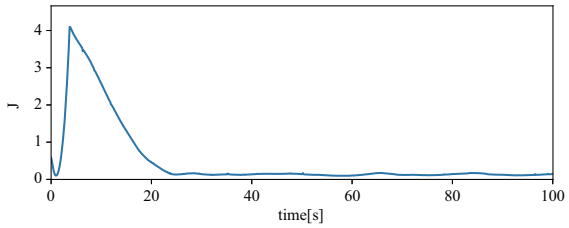

FIGURE 10 The cost function value on prediction horizon p in the real experiment environment at each time step.

It can be seen from Figure 8 that the velocities of CAVs and HDVs in the mixed platoon fluctuate around the equilibrium. Figure 9 shows that in the process of driving, each CAV keeps a smaller inter-vehicle spacing from its predecessor, and the inter-vehicle spacing is not less than 0.05 m all the time. Moreover, we can find that even if the inter-vehicle spacing is smaller, CAVs can still obtain greater acceleration (but within the acceleration limits), which indicates that the emergency capacity of the CAV is better. However, because the calibration errors of the robot vehicles' head orientation and positioning errors affect the calculation of inter-vehicle spacing, the inter-vehicle spacing of HDVs and CAVs fluctuate around 0.408 m and 0.27 m, which are close to the desired inter-vehicle spacing.

The value of cost function J with time in the experiment is shown in Figure 10, which is calculated by all vehicles' state errors and control inputs of all CAVs on the whole prediction horizon p. Figure 10 shows that when the velocity of the leading vehicle gradually reaches the steady state, J tends to a small constant close to zero, indicating that the DMPC algorithm is effective in achieving the platoon control objective.

In addition, the sampling period is set as 0.3 s, and we record that the maximum single step running time of a turnlebot3 controller is 0.237 s, which includes 0.2 s for data receiving from motion capture system and 0.037 s for the maximum single step calculation time of a DMPC controller. However, when the CMPC algorithm is applied to the mixed vehicle platoon control, we find that the single step running time of the controller is as high as 0.342 s, which inevitably results in that the real-time control cannot be guaranteed.

In conclusion, numerical simulation and experimental results have verified that the proposed DMPC algorithm can reduce the computation cost remarkably and ensure the control performance comparable to the CMPC algorithm.

5 | CONCLUSION

In this paper, we have proposed a DMPC algorithm based on the ADMM for a mixed vehicle platoon consisting of an arbitrary sequence of HDVs and CAVs. We have established a generic modeling approach for the arbitrarily mixed vehicle platoon by dividing it into multiple interrelated sub-platoons. Then we have designed a local MPC controller for each sub-platoon, and applied the ADMM to make local MPC controllers coordinate to obtain optimal control inputs for all CAVs in the mixed vehicle platoon from a global perspective. We have finally presented numerical simulations and experiments to verify the effectiveness and superiority of the proposed DMPC algorithm, revealing that control performance is almost the same as that of the CMPC and the computational cost is greatly reduced. A pressing topic for our future work is to further investigate the cooperative predictive control problem for mixed vehicle platoons with disturbances.

AUTHOR CONTRIBUTIONS

Jingyuan Zhan: Formal analysis, funding acquisition, investigation, writing - review and editing. Zhen Hua: Methodology, validation, writing - original draft. Liguo Zhang: Conceptualization, data curation, funding acquisition, project administration, supervision.

ACKNOWLEDGEMENTS

This work is supported by the National Natural Science Foundation of China (NSFC, Grant Nos. U2233211, 62273014 and 61873007), the Beijing Nova Program (No. 20220484133), the Beijing municipal college faculty construction plan for outstanding young talents (No. BPHR202203011), and the Scientific Research Plan of Beijing Municipal Education Commission (No. KM202310005032).

CONFLICT OF INTEREST STATEMENT

The authors have declared no conflict of interest.

DATA AVAILABILITY STATEMENT

Data sharing not applicable to this article as no datasets were generated or analysed during the current study.

ORCID

Jingyuan Zhan https://orcid.org/0000-0002-6863-9252

REFERENCES

1. Maiti, S., Winter, S., Kulik, L., Sarkar, S.: The impact of flexible platoon formation operations. IEEE Trans. Intell. Veh. 5(2), 229–239 (2020)
2. Xu, L., Wang, L.Y., Yin, G., Zhang, H.: Communication information structures and contents for enhanced safety of highway vehicle platoons. IEEE Trans. Veh. Technol. 63(9), 4206–4220 (2014)
3. Kasture, P., Nishimura, H.: Platoon definitions and analysis of correlation between number of platoons and jamming in traffic system. IEEE Trans. Intell. Transp. Syst. 22(1), 319–328 (2021)
4. Guo, X., Wang, J., Liao, F., Teo, R.S.H.: CNN-based distributed adaptive control for vehicle-following platoon with input saturation. IEEE Trans. Intell. Transp. Syst. 19(10), 3121–3132 (2018)
5. Ma, F., Wang, J., Zhu, S., Gelbal, S.Y., Yang, Y., Aksun-Guvenc, B., Guvenc, L.: Distributed control of cooperative vehicular platoon with nonideal communication condition. IEEE Trans. Veh. Technol. 69(8), 8207–8220 (2020)
6. Hu, Y., Chen, C., He, J., Yang, B.: Eco-platooning for cooperative automated vehicles under mixed traffic flow. IEEE Trans. Intell. Transp. Syst. 22(4), 2023–2034 (2021)
7. Wang, S., Yu, B., Wu, M.: MVCM car-following model for connected vehicles and simulation-based traffic analysis in mixed traffic flow. IEEE Trans. Intell. Transp. Syst. 1–8 (2021)
8. Cao, Z., Lu, L., Chen, C., Chen, X.: Modeling and simulating urban traffic flow mixed with regular and connected vehicles. IEEE Access 9, 10392–10399 (2021)
9. Huang, M., Jiang, Z.-P., Ozbay, K.: Learning-based adaptive optimal control for connected vehicles in mixed traffic: Robustness to driver reaction time. IEEE Trans. Cybern. 99, 1–11 (2020)
10. Zhu, W.-X., Zhang, H.M.: Analysis of mixed traffic flow with human-driving and autonomous cars based on car-following model. Phys. A 496, 274–285 (2018)
11. J. I.Ge and Orosz, G.: Optimal control of connected vehicle systems with communication delay and driver reaction time. IEEE Trans. Intell. Transp. Syst. 18(8), 2056–2070 (2017)
12. Gao, W., Jiang, Z.-P., Ozbay, K.: Data-driven adaptive optimal control of connected vehicles. IEEE Trans. Intell. Transp. Syst. 18(5), 1122–1133 (2017)
13. Jiang, L., Ji, J., Ren, Y., Wang, H., Huang, Y.: Risk modeling and quantification of a platoon in mixed traffic based on the mass-spring-damper model. J. Adv. Transp. 2020(12), 1–12 (2020)
14. Huang, M., Gao, W., Jiang, Z.-P.: Connected cruise control for a platoon of human-operated and autonomous vehicles using adaptive dynamic programming. In: 2017 36th Chinese Control Conference, pp. 9478–9483. IEEE, Piscataway (2017)
15. Fiengo, G., Lui, D.G., Petrillo, A., Santini, S., Tufo, M.: Distributed robust PID control for leader tracking in uncertain connected ground vehicles with V2V communication delay. IEEE ASME Trans. Mechatron. 24(3), 1153–1165 (2019)
16. Li, H., Wu, H., Gulati, I., Ali, S.A., Pickert, V., Dlay, S.: An improved sliding mode control (SMC) approach for enhancement of communication delay in vehicle platoon system. IET Intell. Transp. Syst. 16(7), 958–970 (2022)
17. Zhan, J., Ma, Z., Zhang, L.: Data-driven modeling and distributed predictive control of mixed vehicle platoons. IEEE Trans. Intell. Veh. 8(1), 572–582 (2022). https://doi.org/10.1109/TIV.2022.3168591
18. Zheng, H., Wu, J., Wu, W., Negenborn, R.R.: Cooperative distributed predictive control for collision-free vehicle platoons. IET Intell. Transp. Syst. 13(5), 816–824 (2019)
19. Xu, M., Luo, Y., Kong, W., Li, K.: A distributed model predictive control method combined with delay compensator for multiple vehicle platoons. IET Intell. Transp. Syst. 17(2), 357–372 (2022). https://doi.org/10.1049/itr2.12263
20. Liu, X., Ma, K., Kumar, P.R.: Towards provably safe mixed transportation systems with human-driven and automated vehicles. In: 2015 54th IEEE Conference on Decision and Control (CDC), pp. 4688–4694. IEEE, Piscataway (2015)
21. Feng, S., Song, Z., Li, Z., Zhang, Y., Li, L.: Robust platoon control in mixed traffic flow based on tube model predictive control. IEEE Trans. Intell. Veh. 6(4), 711–722 (2021)
22. Luo, Q., Nguyen, A.-T., Fleming, J., Zhang, H.: Unknown input observer based approach for distributed tube-based model predictive control of heterogeneous vehicle platoons. IEEE Trans. Veh. Technol. 70(4), 2930–2944 (2021)
23. Zhao, W., Ngoduy, D., Shepherd, S., Liu, R., Papageorgiou, M.: A platoon based cooperative eco-driving model for mixed automated and human-driven vehicles at a signalised intersection. Transport. Res. C-Emerg. Technol. 95, 802–821 (2018)
24. Gong, S., Du, L.: Cooperative platoon control for a mixed traffic flow including human drive vehicles and connected and autonomous vehicles. Transport. Res. Part B: Methodolog. 116, 25–61 (2018)
25. Boyd, S., Parikh, N., Chu, E., Peleato, B., Eckstein, J.: Distributed optimization and statistical learning via the alternating direction method of multipliers. Found. Trends Mach. Learn. 3(1), 1–122 (2010)
26. Iutzeler, F., Bianchi, P., Ciblat, P., Hachem, W.: Explicit convergence rate of a distributed alternating direction method of multipliers. IEEE Trans. Automat. Contr. 61(4), 892–904 (2016)
27. Treiber, M., Hennecke, A., Helbing, D.: Congested traffic states in empirical observations and microscopic simulations. Phys. Rev. E 62(2), 1805–1824 (2000)
28. Kesting, A., Treiber, M., Helbing, D.: Enhanced intelligent driver model to access the impact of driving strategies on traffic capacity. Philos. Trans. A Math Phys. Eng. 368(1928), 4585–4605 (2010)

How to cite this article: Zhan, J., Hua, Z., Zhang, L.: Cooperative predictive control for arbitrarily mixed vehicle platoons with guaranteed global optimality. IET Intell. Transp. Syst. 17, 1702–1714 (2023). https://doi.org/10.1049/itr2.12363